

# A refractometer based on a micro-slot in a fiber Bragg grating formed by chemically assisted femtosecond laser processing

Kaiming Zhou, Yicheng Lai, Xianfeng Chen, Kate Sugden, Lin Zhang, Ian Bennion

Photonic Research Group, Aston University, Birmingham, U.K.  
[k.zhou@aston.ac.uk](mailto:k.zhou@aston.ac.uk)

**Abstract:** A liquid core waveguide as a refractometer is proposed. Micro-tunnels were created in standard optical fiber using tightly focused femtosecond laser inscription and chemical etching. A 1.2(h)×125(d)×500(l) μm micro-slot engraved along a fiber Bragg grating (FBG) was used to construct liquid core waveguide by filling the slot with index matching oils. The device was used to measure refractive index and sensitivity up to 10<sup>6</sup>/pm was obtained.

©2007 Optical Society of America

**OCIS codes:** (060.2370) Fiber optics sensors, (060.3735) Fiber Bragg gratings, (140.3440) Laser-induced breakdown, (160.2750) Glass and other amorphous materials

---

## References and links

1. V. Bhatia and A. M. Vengsarkar, "Optical fiber long-period grating sensors," *Opt. Lett.* **21**, 692-694 (1996).
2. K. Zhou, L. Zhang, X. Chen and I. Bennion, "Optic sensors of high refractive-index responsivity and low thermal cross sensitivity that use fiber Bragg gratings of >80° tilted structures," *Opt. Lett.* **31**, 1193-1195 (2006).
3. C. -F. Chan, C. Chen, A. Jafari, A. Laronche, D. J. Thomson and J. Albert, "Optical fiber refractometer using narrowband cladding-mode resonance shifts," *Appl. Opt.* **46**, 1142-1149 (2007).
4. A. Iadicco, A. Cusano, A. Cutolo, R. Bernini and M. Giordano, "Thinned fiber Bragg gratings as high sensitivity refractive index sensor," *IEEE Photon. Technol. Lett.* **16**, 1149-1151 (2004).
5. M. Holtz, P. K. Dasgupta, G. Zhang, "Small-volume Raman spectroscopy with a liquid core waveguide," *Anal. Chem.* **71**, 2934 -2938 (1999).
6. M. Brown, T. Vestad, J. Oakey and D. W. M. Mar, "Optical waveguides via viscosity-mismatched microfluidic flows," *Appl. Phys. Lett.* **88**, 134109 (2006).
7. M. C. Phan Huy, G. Laffont, V. Dewynter, P. Ferdinand, P. Roy, J. -L. Auguste, D. Pagnoux, W. Blanc, and B. Dussardier, "Three-hole microstructured optical fiber for efficient fiber Bragg grating refractometer," *Opt. Lett.* **32**, 2390-2392 (2007).
8. F. M. Cox, A. Argyros, and M. C. J. Large, "Liquid-filled hollow core microstructured polymer optical fiber," *Opt. Express* **14**, 4135-4140 (2006).
9. K. Davis, K. Miura, N. Sugimoto, K. Hirao, "Writing waveguides in glass with a femtosecond laser", *Opt. Lett.* **21**, 1729-1731 (1996).
10. C. B. Schaffer, A. Brodeur, J. F. García, and E. Mazur, "Micromachining bulk glass by use of femtosecond laser pulses with nanojoule energy," *Opt. Lett.* **26**, 93-95 (2001).
11. C. Hnatovsky, R. S. Taylor, E. Simova, V. R. Bhardwaj, D. M. Rayner, and P. B. Corkum, "Polarization-selective etching in femtosecond laser-assisted microfluidic channel fabrication in fused silica," *Opt. Lett.* **30**, 1867-1869 (2005).
12. Y. Lai, K. Zhou, L. Zhang and I. Bennion, "Microchannels in conventional single-mode fibers," *Opt. Lett.* **31**, 2559-2561 (2006).
13. C. Hensley, D. H. Broaddus, C. B. Schaffer, and A. L. Gaeta, "Photonic band-gap fiber gas cell fabricated using femtosecond micromachining," *Opt. Express* **15**, 6690-6695 (2007).
14. A. van Brakel, C. Grivas, M. N. Petrovich, and D. J. Richardson, "Micro-channels machined in microstructured optical fibers by femtosecond laser," *Opt. Express* **15**, 8731-8736 (2007).
15. X. Chen, K. Zhou, L. Zhang and I. Bennion, "Optical chemsensors utilizing long-period fiber gratings UV-inscribed in D-fiber with enhanced sensitivity through cladding etching," *Photon. Technol. Lett.* **16**, 1352-1354 (2004).

## 1. Introduction

Using a fiber grating as the basis for a refractometer is attractive in applications where in-situ monitoring or sensor miniaturization is demanded. In terms of mode coupling, three approaches have been employed to realize such a refractometer: (a) forward cladding mode coupling which involves long period gratings (LPGs) [1] or tilted fiber Bragg grating (TFBG) with large tilting angles [2], (b) backward cladding mode coupling generated by FBGs or TFBGs with small tilt angles [3], or (c) backward core mode coupling which requires the fiber's cladding being removed [4]. Devices of the first category give the biggest sensitivities but they are limited in respect of miniaturization because they use transmission and are usually several centimeters long. For those using backward cladding mode coupling, the sensitivity is relatively low with typical value around  $\sim 10^{-4}/\text{pm}$ . For the third option, with the removal of the cladding, the devices are extremely fragile and need to be packaged which inevitably adds to their size. For all of these methods, only a small portion of the light propagating in the fiber - the evanescent wave - interacts with the material under test, making the sensitivity of the device limited. In addition, the evanescent wave can only exist in the cladding and the operational range is thus limited to refractive indices below that of the fiber core.

An intuitive way to enhance the sensitivity is to use the liquid as the core of a waveguide instead of its cladding. Liquid has been used for guiding light in pursuing a range of purposes, like spectroscopy [5] and fluorescence [6] etc, but fiber-based liquid core devices using a grating to interrogate refractive index (RI) have not been reported yet so far to our best knowledge. Traditional optical fibers with a solid core seem unsuitable in this respect and microstructure optical fibers (MOF) appear as the only option. MOFs have been reported interacting with liquids either still using the evanescent wave [7] or guiding light in liquid-filled hollow core [8]. But writing FBGs in MOFs is not trivial, it is either impractical because of the huge hollow core [8] or requires special preparation of photosensitive fiber [7]. Most reported MOF based liquid or gas sensors also incur difficulties in pumping the measurands to the functional region of the fiber. It has always been desirable therefore to open bypassing tunnels across the fiber at the required locations but due to their small sizes and chemical inertness, in most optical fibers it has been hard to obtain holes with high aspect ratios.

Recently, techniques using tightly focused femtosecond (fs) laser pulses to produce micro-structures in silica/glass materials have become the focus of research interest. Such processes have been used to induce refractive changes for writing optical waveguides [9] and, with the aid of chemical etching, have been applied in micromachining [10]. It has been reported that regions treated by the fs laser exhibit a remarkably high etching rate compared to pristine material, with contrast ratios up to 100:1 [11]. Most reports so far still focus on planar devices and only a few addressed engraving in optical fiber [12][13][14]. It is believed that this technique provides the solution to the issues described above, by not only creating bypass tunnels to MOFs, but also providing the opportunity to realize microstructures locally within the cores of traditional optical fibers, making them competitive with MOFs.

In this paper, we report on fabrication of micro tunnels within standard optical fibers using a chemically assisted fs laser process. The liquid refractive index (LRI) sensitivity was tested with a  $1.2 \times 125 \times 500 \mu\text{m}$  micro-slot engraved along a FBG which takes advantage of a liquid core waveguide and is more robust compared to cladding removed sensors [3] since the majority of the cladding still remains. Moreover, such a device works with both low and high LRIs, and shows a much higher sensitivity in the high RI regime. Modeling of the liquid core waveguide was carried out and the simulation results are in excellent agreement with the experiment.

## 2. Device description and numerical analysis

Figure 1 shows the geometry of the micro-slot engraved along an FBG. With an opening on both sides, the liquid needs only to travel the radius of the fiber to fill the slot and form the

liquid core slab waveguide. Here we use the liquid core waveguide as a refractometer to test LRI. To maximize the interaction between the optical signals propagating in the core and the

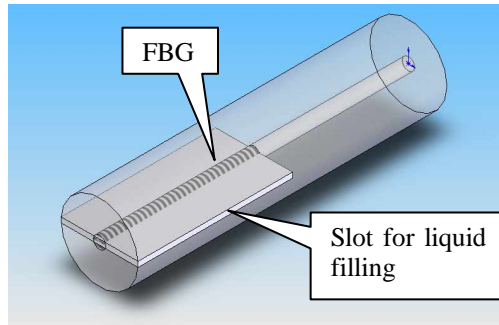


Fig. 1. Geometry of a micro-slot across the optical fiber.

liquid, the slot was purposely built across the core. With commercial software, FEMLAB, we simulated its performance. Figure 2(a) plots its effective index against LRI. In the simulation the radius and RI of the fiber are  $62.5\mu\text{m}$  and 1.44403 for the cladding and  $4.15\mu\text{m}$  and 1.4512 for the core, respectively. For a given slot, two regions with very different slopes can be seen with the changeover around RI of the fiber material. By examining the evolution of the field distribution (Fig. 2(b) or the online movie) with respect to the LRI, we can gain a clearer understanding of the difference between these two regions. In the low LRI region, light is still confined in the glass and only evanescent wave penetrates into the liquid while for the higher LRIs, the light exists mainly in the liquid and the effective index is decided by the liquid. The influence of the opening size of the slot is also illustrated in Fig. 2(a) and larger slot presents a higher sensitivity to LRI.

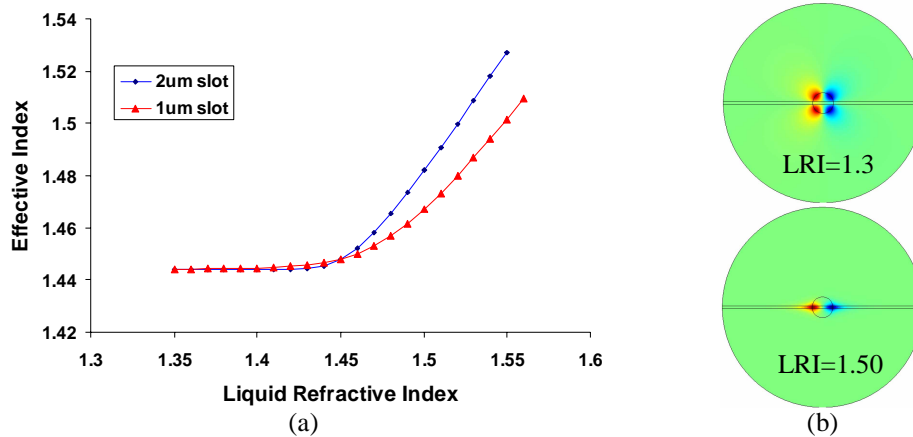


Fig. 2. (a) Effective index of the slotted optical fiber against RI of the filling liquid. (b) Field distribution of the fundamental mode of the liquid core slab waveguide for different LRI (also shown in the online movie).

### 3. Engraving of the micro-structures in optical fiber

In the experiment, fs pulses ( $\lambda = 800\text{nm}$ ) were tightly focused on the fiber by a  $\times 100$  objective lens with N.A. of 0.55 and a working distance of 13mm. The pulse width of the laser was  $\sim 150\text{fs}$  with 1kHz repetition rate. The fiber was mounted on a dual-axis air-bearing translation stages so that the desired pattern could be written by translating the fiber with respect to the fs-laser beam. If the inscription was carried out with the optical fiber in the air there was distortion to the focus volume of the laser beam [12]. This effect is caused by the cylindrical

geometry of the fiber and is more pronounced as the focus volume moved deeper into the fiber, limiting the depth of inscription. As Fig. 3(a) shows, the focused laser only left a track on the front part of its traveling path for a through line across the fiber. When it ran closer to the core, the focus volume was expanded, yielding a broader but shallower modification to the glass which gradually disappeared. The deepest distance where the fs exposure still worked depended on the energy of the laser pulse but generally it was limited to within only half of the fiber's diameter. To circumvent the cladding's curvature, a glass slip was placed on top of the fibre and index-matched to the fiber with oil as Fig. 3(b) discloses. The focus spot was then freely moved within the fiber without being distorted. Shown in Fig. 3(c) is a much more well-defined through line made with this way.

Following the fs-laser inscription, the fiber with the patterned microstructure was chemically etched in a 5% HF acid solution. An ultrasonic bath was used to enhance the penetration of HF acid into the fs-modified area. The transmission and reflection was monitored using an optical spectrum analyzer (OSA) and a broadband source during the etching process. Figure 4 gives the recorded transmission during the etching process for a straight line. Loss appeared after 9 minutes of etching and then increased at a very fast rate, indicating that area close to the core was being etched. We estimated that the etching rate for the modified fiber was roughly  $7\mu\text{m}/\text{min}$ , 100 times higher than that of the non-exposed fiber [15].

We then patterned a  $125\times 500\mu\text{m}$  rectangle by scanning the focus of the laser beam 2-dimensionally. Low pulse energies can be used to give smaller openings, provided that they are still strong enough to induce material modification. The structure was made according to Fig. 1 to coincident with a  $400\mu\text{m}$  long FBG to minimize the device size. Following etching, a micro-slot with opening height of  $1.2\mu\text{m}$  was produced as Fig. 5(a) shows, revealing a high contrast ratio of about 100:1. Though already with two openings at the top and bottom of the slot, cleaving of the fibre at one end of the device was also used to enhance the exchangeability of substance in the slot and also make it easier to operate the device. Fig. 5(b) gives the spectral evolution of the FBG during the etching process, showing blue shift of the Bragg wavelength and decreasing of the transmission.

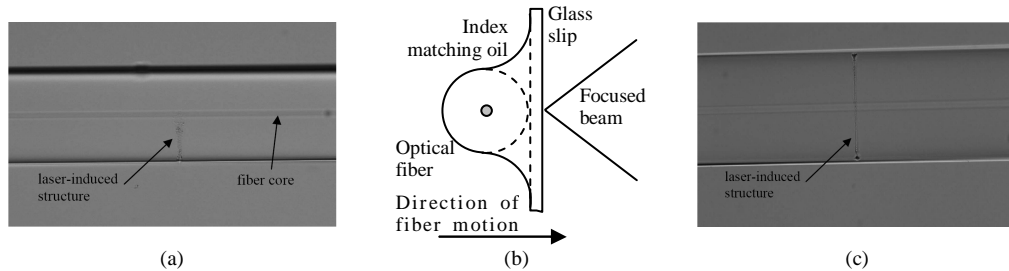


Fig. 3. A through line written with the fs laser when the optical fiber is in (a) air and in (c) index matching oil. (b) The configuration using an adaptive glass slip and index matching oil

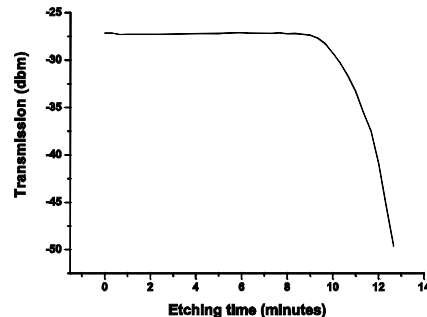


Fig. 4. (a) Transmission loss against time as the microstructure was etched.

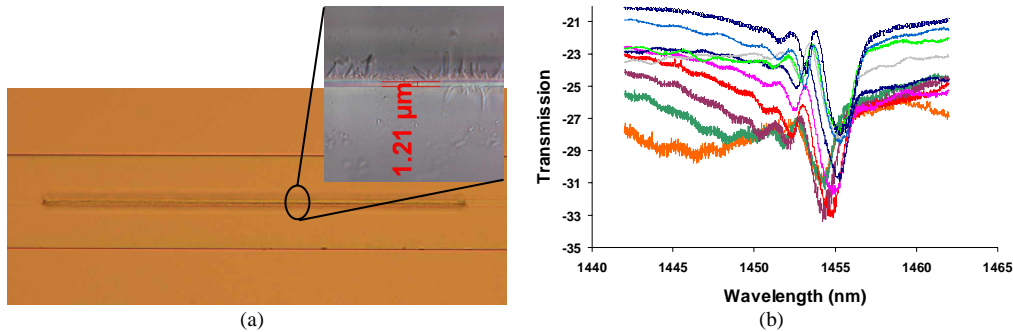


Fig. 5. (a) The 1.2 $\mu\text{m}$  high micro-slot engraved in standard optical fiber with fs inscription and chemical etching. (b) Spectral evolution of the FBG during the fiber was etched, with top one as the initial state and the bottom one as finish state.

#### 4. RI sensing and discussion

The response of the FBG/micro-slot device to LRI was tested with a series of index matching oils (from Cargille Laboratories) by immersing the device tip in the oil and the reflection spectrum was monitored with an OSA. After each oil sample was measured, the device was rinsed with acetone, methanol and water in turn for several times until the original spectrum was restored, making sure no residue oil left in the slot. Shown in Fig. 6(a) and 6(b) are the spectra of the grating for the successively increased LRI. In agreement with simulation results in section 2, two distinguishable regimes can be seen with a boundary around an index of 1.46. Initially only the main Bragg peak appears while once above 1.46, new reflection peaks emerge at longer wavelengths as marked by arrows in Fig. 6(b). No reflection from the fiber end was noticed thanks to the small RI difference between the oil and the fiber.

These two regimes can also be distinguished by close examination of the main Bragg peak around 1460nm. Figure 6(c) gives its response to a variation of the LRI in terms of its wavelength and the strength. In the low LRI region, both change almost monotonically with a trend similar to previous reports [3, 7] and the sensitivity reaches 116nm/refractive index unit (RIU) (or  $8.6 \times 10^{-6}$ /pm) for an LRI from 1.44 to 1.46. Once in regime II, the scenario changes substantially, showing obvious less reflectivity and unpredictable wavelength. In this regime, the LRI is larger than that of the fiber with no guiding modes supported by the fiber. The remaining peak should arise from the leaky mode instead of the fundamental guiding mode.

In the high LRI regime, the oil in the slot begins to support propagation modes and their number is dependent on the index of the oil, as indicated by the increasing number of peaks that emerge in the reflection spectrum (Fig. 6(b)). The rightmost peak belongs to the fundamental mode since its effective index is the largest. The enlarged version for different LRI is shown in the inset of Fig. 6(b) to give a clearer view and it can be seen that, with increasing of LRI, the peak gradually becomes broader with full width half amplitude changed from 1.6nm for LRI of 1.478 to 5.9nm for 1.55. At the same time, the strength of the peak decreases, caused by the decreasing coupling from the un-etched fiber section. This could be improved by implementing a round tunnel in the central portion of the slot with the same fs inscription and chemical etching method, and in this way it may be possible to realize a single mode liquid core waveguide.

More exciting is about the wavelength shift of the peak with changing of LRI as revealed by the hollow diamonds in Fig. 6(d), revealing a very linear relationship. Using simulated effective indices for a 1 $\mu\text{m}$  slot of Fig. 2(a), the Bragg wavelengths were also calculated and the results shown as blue squares in Fig. 6(d) exhibit excellent agreement with the experiment in terms of the slope. The offset may arise from the dispersion of the oil since their indices are given for visible light instead of the infrared. Theoretically the turning point for these two regimes is the RI of the fiber core, i.e. 1.45, while it is 1.46 experimentally and the difference should be the dispersion of the oil from the visible wavelength to the infrared. With this

amending, better overlaps with the experimental result was obtained, as shown by red stars in Fig. 6(d). Evaluation of another device which used a 1550nm FBG was also performed and the results are included in Fig. 6(d), with the average sensitivity of 945nm/RIU ( $1.0 \times 10^{-6}$ /pm). Figure 6(e) gives the sensitivity for the Bragg peak of the fundamental mode in low and high LRI regimes. Apparently, much higher sensitivity is shown in the high LRI region.

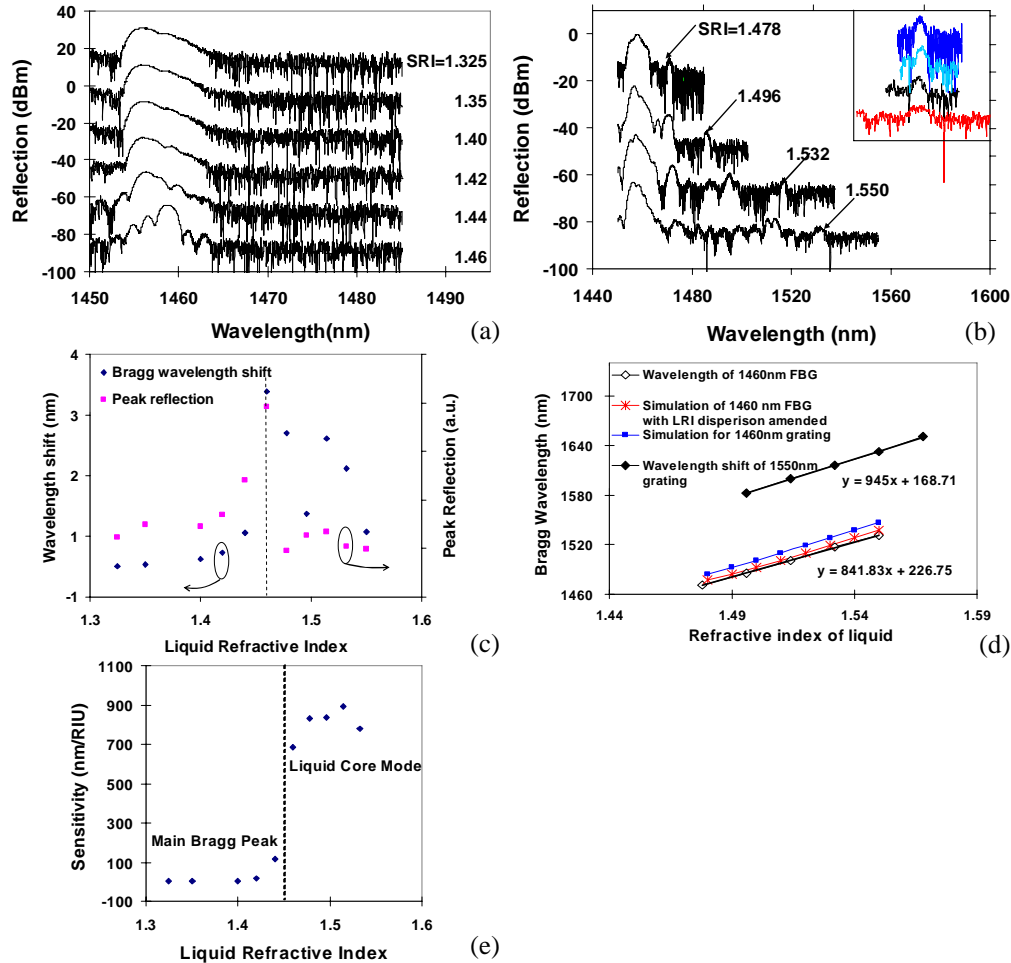


Fig. 6. Reflection spectra of the micro-slot/FBG device when the RI of the oil is (a) below and (b) above that of optical fiber. Arrows in (b) locate the rightmost Bragg peak (corresponding to the fundamental mode) of the liquid core waveguide and the inset focuses on these peaks. (c) Wavelength shift and variation of the amplitude of the main Bragg peak with respect to RI of the oil. (d) Experimental and simulated wavelength shift of the liquid core FBGs. (e) Sensitivity of the device over the low RI and high RI regime.

## 5. Conclusions

A micro-slot through the fiber device was proposed to test RI of liquids. Simulation results show the device is effective in a broad RI range and presents improved sensitivity over previously reported work. Chemical etching assisted fs laser inscription technique was used to create a  $1.2 \times 125 \times 500 \mu\text{m}$  micro-slot across an FBG, which was then used as a refractometer to test the RI of oils. Compared to evanescent wave based refractometers, the working RI range of the device is extended to 1.55 and sensitivity up to 945nm/RIU (or  $1.0 \times 10^{-6}$ /pm) is achieved, which is comparable to LPG sensors. The device has great potential in medical, chemical sensing applications.